Approaching Minimum Time Control of Timed Continuous Petri nets ⋆

Hanife Apaydin-Özkan, * **Jorge Júlvez,** * **Cristian Mahulea,** * **Manuel Silva** *

* *Instituto de Investigación en Ingeniería de Aragon (I3A), Universidad de Zaragoza, Spain (e-mails: hapaydin, julvez, cmahulea, silva@unizar.es)*

Abstract: This paper considers the problem of controlling timed continuous Petri nets under infinite server semantics. The proposed control strategy assigns piecewise constant flows to transitions in order to reach the target state. First, by using linear programming, a method driving the system from the initial to the target state through a linear trajectory is developed. Then, in order to improve the time of the trajectory, intermediate states are added by means of bilinear programming. Finally, in order to handle potential perturbations, we develop a closed loop control strategy that follows the trajectory computed by the open loop control by calculating a new state after each time step. The algorithms developed here are applied to a manufacturing system.

Keywords: Timed continuous Petri nets, minimum time control, piecewise linear trajectory

1. INTRODUCTION

Petri nets (PNs) are frequently used for modeling, analysis and synthesis of discrete event systems. The distributed state or marking of a PN is given by a vector of natural numbers which represent the number of tokens in each place. Similarly to most formalisms for discrete event systems, PNs suffer from the *state explosion problem*. One possible way to overcome this problem is *fluidification*, a classical relaxation technique.

Continuous Petri nets are a fluid approximation of classical discrete Petri nets (David and Alla (2005); Silva and Recalde (2004)). Unlike conventional PNs, a transition in a continuous Petri net can be fired in a "non negative real" quantity. This leads to continuous markings instead of discrete ones. Similarly to discrete PNs, time delays can be associated to the firing of transitions, the resulting net is called *timed continuous Petri net* (contPN).

As in discrete PNs, different server semantics can be adopted for the firing of transitions. Among them the most widely used semantics are *finite server* and *infinite server*. In Mahulea et al. (2009), it is shown that infinite server semantics provides a better approximation of the steady state throughput than finite server semantics for a wide class of Petri nets under some general conditions.

A contPN system with infinite server semantics is a subclass of *Piecewise Linear Systems* (PWL), with input constraints. A PWL system is composed of several linear subsystems together with switching rules (Bemporad and Morari (1999)). Many works deal with stability analysis or control law design of such systems (Montagner et al. (2006); Yang et al. (2006); Habets et al. (2006); Balduzzi et al. (2000)). However, most of these methods cannot be directly applied to contPNs, because of their particular dynamic input constraints.

Control of contPNs with infinite server semantics has already been considered in the literature. In Mahulea et al. (2008b) it is shown that, the optimal steady state control problem of timed contPN system can be solved by means of *Linear Programming Problem* (LPP) when all transitions are assumed to be controllable. The transitory control problem is also considered by means of implicit and explicit MPC control strategy (Mahulea et al. (2008a)). A Lyapunov-function-based dynamic control algorithm was proposed in (Xu et al. (2008)), which can ensure global convergence of both system states and input signals. In contrast to the method in this last work, where step plus ramp trajectories under closed loop control are considered, the technique proposed in this paper for the computation of a control law for direct linear trajectory is based on linear programming instead of nonlinear programming. This implies that the complexity of this new approach is significantly lower given that it can be solved in polynomial time. Interestingly, the time of the obtained trajectories by both methods are very similar in general. The method in Xu et al. (2008) introduces the notion of intermediate states, leading to a piecewise linear trajectory that is computed by solving a *BiLinear Programming Problem* (BLP).

⋆ This work was partially supported by CICYT - FEDER projects DPI2006-15390, TIN2007-66523, and by the European Community Seventh Framework Programme under project DISC (Grant Agreement n. INFSO-ICT-224498). The work of H.Apaydin-Özkan was supported in part by the Diputacin General de Aragón for 15 months stay in the Group of Zaragoza; on leave from Faculty of Electrical and Electronics Engineering, Anadolu University, Eskisehir, Turkey. This paper has been written in honor to Prof. L. Recalde, who passed away last December.

In this work, we extend the control strategy presented in Apaydin-Ozkan et al. (2009) which aims at driving the system from an initial state to a target one by minimizing the time of a linear trajectory. The proposed strategy computes first the control actions to drive the system to the target state through a straight line (Section 3). Such control actions are the result of solving a LPP. Then, in Section 4, intermediate states, not necessarily on the line connecting the initial and the target marking, are computed, by means of a BLP, in order to obtain faster trajectories. Moreover, an algorithm that recursively refines the initially obtained trajectory is given. These computations are then used to develop a closed loop scheme which is explained in Section 5. In Section 6, a manufacturing system is taken as a case study and studied to reach a certain marking in minimum time. Finally, some conclusions and future directions are drawn in Section 7.

2. CONTINUOUS PETRI NETS

We assume that the reader is familiar with discrete PNs. In contPN systems, the firing of transitions is not restricted to the natural numbers but to the nonnegative real numbers.

2.1 Timed Continuous Petri nets

Definition 1. A continuous PN system is a pair $\langle \mathcal{N}, \boldsymbol{m}_0 \rangle$ where $\mathcal{N} = \langle P, T, \boldsymbol{Pre}, \boldsymbol{Post} \rangle$ is the net structure with the set of places P, the set of transitions T, pre and post matrices $\boldsymbol{Pre}, \boldsymbol{Post} \in \mathbb{R}_{\geq 0}^{|P| \times |T|}$, and $\boldsymbol{m}_0 \in \mathbb{R}_{\geq 0}^{|P|}$ as the initial state.

Let p_i, $i = 1, \ldots, |P|$ and $t_j, j = 1, \ldots, |T|$ denote the places and transitions. For a place $p_i \in P$ and a transition $t_j \in T$, Pre_{ij} and $Post_{ij}$ represent the weights of the arcs from p_i to t_j and from t_j to p_i, respectively. Each place p_i has a marking denoted by $m_i \in \mathbb{R}_{\geq 0}$. The vector of all token loads is called *state* or *marking*, and is denoted by $\boldsymbol{m} \in \mathbb{R}_{\geq 0}^{|P|}$. For every node $v \in P \cup T$, the sets of its input and output nodes are denoted as ${}^\bullet v$ and $v^\bullet$, respectively.

A transition $t_j \in T$ is enabled at $\boldsymbol{m}$ iff $\forall p_i \in {}^\bullet t_j$, $m_i > 0$ and its enabling degree is given by

$$enab(t_j, \boldsymbol{m}) = \min_{p_i \in {}^\bullet t_j} \left\{ \frac{m_i}{Pre_{ij}} \right\}$$

which represents the maximum amount in which t_j can fire. An enabled transition t_j can fire in any real amount α, with $0 < \alpha \leq enab(t_j, \boldsymbol{m})$ leading to a new state $\boldsymbol{m'} = \boldsymbol{m} + \alpha \cdot \boldsymbol{C}_{\cdot j}$ where $\boldsymbol{C} = \boldsymbol{Post} - \boldsymbol{Pre}$ is the token flow matrix and $\boldsymbol{C}_{\cdot j}$ is its j^{th} column. If $\boldsymbol{m}$ is reachable from $\boldsymbol{m}_0$ through a finite sequence σ, the state (or fundamental) equation is satisfied: $\boldsymbol{m} = \boldsymbol{m}_0 + \boldsymbol{C} \cdot \boldsymbol{\sigma}$, where $\boldsymbol{\sigma} \in \mathbb{R}_{\geq 0}^{|T|}$ is the firing count vector, i.e., σ_j is the cumulative amount of firings of t_j in the sequence σ.

Under any time interpretation, the state equation has an explicit dependence on time, denoted by τ: $\boldsymbol{m}(\tau) = \boldsymbol{m}_0 + \boldsymbol{C} \cdot \boldsymbol{\sigma}(\tau)$ which through time differentiation becomes $\dot{\boldsymbol{m}}(\tau) = \boldsymbol{C} \cdot \dot{\boldsymbol{\sigma}}(\tau)$. The derivative of the firing sequence $\boldsymbol{f}(\tau) = \dot{\boldsymbol{\sigma}}(\tau)$ is called the firing flow. Depending on how the flow is defined, different firing semantics appear, being the most used ones *infinite* and *finite* server semantics.

This paper deals with infinite server semantics for which the flow of a transition t_j is defined as:

$$f_j(\tau) = \lambda_j \cdot enab(t_j, \boldsymbol{m}(\tau)) = \lambda_j \cdot \min_{p_i \in {}^\bullet t_j} \left\{ \frac{m_i(\tau)}{Pre_{ij}} \right\} \quad (1)$$

where λ_j is a constant value representing the firing rate of transition t_j. Since the flow of a transition depends on its enabling degree which is based on the minimum function, a timed contPN with infinite server semantics is a PWL system with polyhedral regions and everywhere continuous vector field. The state space (or reachability set) $\mathcal{R}$ of a contPN system can be divided into regions (disjoint except possibly on the borders), as follows: $\mathcal{R} = \mathcal{R}^1 \cup ... \cup \mathcal{R}^\gamma$ where $\gamma \leq \prod_{j=1}^{|T|} |{}^\bullet t_j|$. Intuitively, each $\mathcal{R}^z$ denotes a region where the flow is limited by the same subset of places (one for each transition). More formally, two markings m_a and m_b belong to the same region $\mathcal{R}^z$ iff $[\forall\, t \in T$ and $\forall\, p_u, p_v \in {}^\bullet t$ it holds that $m_a(p_u) \leq m_a(p_v) \leftrightarrow m_b(p_u) \leq m_b(p_v)]$.

For a given $\mathcal{R}^z$, we can define the constraint matrix $\boldsymbol{\Pi}^z \in \mathbb{R}_{\geq 0}^{|P|}$ as follows. Let $\boldsymbol{m}$ be an interior point of $\mathcal{R}^z$, then $\boldsymbol{\Pi}^z$ is defined as:

$$\boldsymbol{\Pi}^z_{ji} = \begin{cases} \dfrac{1}{Pre_{ij}}, \; if \;\; \dfrac{m_i}{Pre_{ij}} = \min\limits_{p_h \in {}^\bullet t_j} \left\{ \dfrac{m_h}{Pre_{hj}} \right\} \\ 0, \qquad \text{otherwise} \end{cases} \quad (2)$$

If marking $\boldsymbol{m}$ belongs to $\mathcal{R}^z$, we denote $\boldsymbol{\Pi}(\boldsymbol{m}) = \boldsymbol{\Pi}^z$ the corresponding constraint matrix (if $\boldsymbol{m}$ is a border point and belongs to several regions, $\boldsymbol{\Pi}(\boldsymbol{m})$ is the constraint matrix of any of these regions). In the constraint matrix, each row $j = 1, 2..., |T|$ has only one non-null element in the position i that corresponds to the place p_i that restricts the flow of transition t_j. On the other hand, the firing rate of transitions can also be represented by a diagonal matrix $\boldsymbol{\Lambda} = \text{diag}\{\lambda_1, ...\lambda_{|T|}\}$. Using this notation, the nonlinear flow of the transitions at a given state $\boldsymbol{m}$ is written as:

$$\boldsymbol{f} = \boldsymbol{\Lambda} \cdot \boldsymbol{\Pi}(\boldsymbol{m}) \cdot \boldsymbol{m} \quad (3)$$

Example 2. Let us consider the PN in Figure 1. Assume $\boldsymbol{\lambda} = [4\ 1\ 3\ 1]^T$, $\boldsymbol{m}_0 = [7.5\ 4.5\ 4\ 2\ 1.5\ 5\ 4\ 2.5]^T$ and $\boldsymbol{m}_f = [7\ 5\ 5\ 1\ 1\ 4\ 5\ 3]^T$.

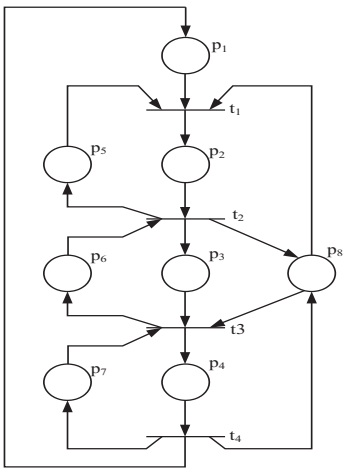

Fig. 1. A PN taken from (Zhou et al. (1990))

Independently of $\boldsymbol{m}_0$, the system dynamics is described as follows:

$$
\begin{aligned}
\dot{m}_1 &= f_4 - f_1 = \lambda_4 \cdot m_4 - \lambda_1 \cdot \min\{m_5, m_1, m_8\} \\
\dot{m}_2 &= f_1 - f_2 = \lambda_1 \cdot \min\{m_5, m_1, m_8\} - \lambda_2 \cdot \min\{m_2, m_6\} \\
\dot{m}_3 &= f_2 - f_3 = \lambda_2 \cdot \min\{m_2, m_6\} - \lambda_3 \cdot \min\{m_3, m_7, m_8\} \\
\dot{m}_4 &= f_3 - f_4 = \lambda_3 \cdot \min\{m_3, m_7, m_8\} - \lambda_4 \cdot m_4 \\
\dot{m}_5 &= f_2 - f_1 = \lambda_2 \cdot \min\{m_2, m_6\} - \lambda_1 \cdot \min\{m_5, m_1, m_8\} \\
\dot{m}_6 &= f_3 - f_2 = \lambda_3 \cdot \min\{m_3, m_7, m_8\} - \lambda_2 \cdot \min\{m_2, m_6\} \\
\dot{m}_7 &= f_4 - f_3 = \lambda_4 \cdot m_4 - \lambda_3 \cdot \min\{m_3, m_7, m_8\} \\
\dot{m}_8 &= f_2 + f_4 - f_1 - f_3 = \lambda_2 \cdot \min\{m_2, m_6\} + \lambda_4 \cdot m_4 \\
&\quad -\lambda_1 \cdot \min\{m_5, m_1, m_8\} - \lambda_3 \cdot \min\{m_3, m_7, m_8\}
\end{aligned} \tag{4}
$$

Note that $\boldsymbol{m}_0$ and $\boldsymbol{m}_f$ are in different regions:

- $\boldsymbol{m}_0 \in \mathcal{R}^1 : \{\boldsymbol{m} \mid m_5 \leq m_1,\ m_5 \leq m_8,\ m_8 \leq m_7,\ m_8 \leq m_3,\ m_2 \leq m_6\}$
- $\boldsymbol{m}_f \in \mathcal{R}^2 : \{\boldsymbol{m} \mid m_5 \leq m_1,\ m_5 \leq m_8,\ m_8 \leq m_7,\ m_8 \leq m_3,\ m_6 \leq m_2\}$

For example, the system dynamics for $\mathcal{R}^1$ is:

$$
\begin{cases}
\dot{m}_1 = m_4 - 4 \cdot m_5 \\
\dot{m}_2 = 4 \cdot m_5 - m_2 \\
\dot{m}_3 = m_2 - 3 \cdot m_8 \\
\dot{m}_4 = 3 \cdot m_8 - m_4 \\
\dot{m}_5 = m_2 - 4 \cdot m_5 \\
\dot{m}_6 = 3 \cdot m_8 - m_2 \\
\dot{m}_7 = m_4 - m_8 \\
\dot{m}_8 = m_2 + m_4 - 4 \cdot m_5 + 3 \cdot m_8
\end{cases} \tag{5}
$$

2.2 Controlled Timed Continuous Petri Nets

In this section, we consider contPN systems subject to external control actions, and assume that the admissible control law can only *slow-down* the firing speed of transitions (Silva and Recalde (2004)). If a transition can be controlled (its flow can be reduced or even stopped), we will say that it is a controllable transition (Mahulea et al. (2008b)). In this work, it will be assumed that all transitions are controllable.

Definition 3. The controlled flow, $\boldsymbol{w}$, of a timed contPN is defined as $\boldsymbol{w}(\tau) = \boldsymbol{f}(\tau) - \boldsymbol{u}(\tau)$, with $0 \leq \boldsymbol{u}(\tau) \leq \boldsymbol{f}(\tau)$, where $\boldsymbol{f}$ is the flow of the uncontrolled system, i.e., defined as in (1), and $\boldsymbol{u}$ is the control action.

Therefore, the control input $\boldsymbol{u}$ is dynamically upper bounded by the flow $\boldsymbol{f}$ of the corresponding unforced system. Under these conditions, the overall behaviour of the system in which all transitions are controllable is ruled by the following system:

$$
\begin{aligned}
&\dot{\boldsymbol{m}} = \boldsymbol{C} \cdot [\boldsymbol{f} \ - \ \boldsymbol{u}] = \boldsymbol{C} \cdot \boldsymbol{w} \\
&0 \leq \boldsymbol{u} \leq \boldsymbol{f}
\end{aligned} \tag{6}
$$

The constraint $0 \leq \boldsymbol{u} \leq \boldsymbol{f}$ can be rewritten as $0 \leq \boldsymbol{f} - \boldsymbol{u} \leq \boldsymbol{f}$. From the definition $\boldsymbol{w} = \boldsymbol{f} - \boldsymbol{u}$ and using (3), the constraint can be expressed as:

$$
0 \ \leq \ \boldsymbol{w} \ \leq \ \boldsymbol{\Lambda} \cdot \boldsymbol{\Pi}(\boldsymbol{m}) \cdot \boldsymbol{m} \tag{7}
$$

The following sections show how to compute a control action $\boldsymbol{u}$ that drives the system from the initial marking $\boldsymbol{m}_0$ to a desired target marking $\boldsymbol{m}_f$. Section 3 describes a method to obtain a linear trajectory. Section 4 makes use of such a method to compute piecewise linear trajectories in order to improve the time to reach $\boldsymbol{m}_f$. Notice that in order to be reachable, $\boldsymbol{m}_f$ necessarily satisfies the state equation, i.e., $\boldsymbol{m}_f = \boldsymbol{m}_0 + \boldsymbol{C} \cdot \boldsymbol{\sigma}$. Our procedure consists of assigning piecewise constant controlled flow $\boldsymbol{w}$ that satisfies dynamic upper bounds. In the sequel, we assume that $\boldsymbol{m}_0$ and $\boldsymbol{m}_f$ are interior points of the reachability space, i.e., the markings are strictly positive. The assumption that $\boldsymbol{m}_0 > 0$ ensures that the system can straightforwardly move at $\tau = 0$ in the direction of $\boldsymbol{m}_f$; the assumption that $\boldsymbol{m}_f > 0$ ensures that $\boldsymbol{m}_f$ can be reached (Júlvez et al. (2003)) in finite time (Mahulea et al. (2008b)).

3. COMPUTATION OF LINEAR TRAJECTORIES

In this section, we will distinguish two cases: (A) $\boldsymbol{m}_0$ and $\boldsymbol{m}_f$ are in the same region and (B) they are in different regions. In this last case the crossing points of the straight line and borders must be considered.

(A) $\boldsymbol{m}_0$ and $\boldsymbol{m}_f$ are in the same region $\mathcal{R}^z$. Then all the states on the straight line connecting them are also interior points of $\mathcal{R}^z$ since all the regions are convex. The following LPP computes the correspondig control law, where $\boldsymbol{x} = \boldsymbol{w} \cdot \tau_f$,

$$
\begin{aligned}
&\min\ \tau_f \\
&\quad \boldsymbol{m}_f = \boldsymbol{m}_0 + \boldsymbol{C} \cdot \boldsymbol{x} \qquad (a) \\
&\quad 0 \leq x_j \leq \lambda_j \cdot \Pi^z_{ji} \cdot \min\left\{m_{0_i}, m_{f_i}\right\} \cdot \tau_f, \\
&\qquad \forall\ j \in \{1, .., |T|\} \text{ where } i \text{ satisfies } \Pi^z_{ji} \neq 0 \ \ (b)
\end{aligned} \tag{8}
$$

The equations correspond to: (a) the time dependent equation of the straight line connecting $\boldsymbol{m}_0$ to $\boldsymbol{m}_f$, (b) derives from the flow constraints in (7). Notice that (8)(b) is a linear constraint because m_{0_i} and m_{f_i} are known.

(B) $\boldsymbol{m}_0$ and $\boldsymbol{m}_f$ are in different regions. The line connecting $\boldsymbol{m}_0$ and $\boldsymbol{m}_f$ can be divided in several segments, each one starting in a border (or in $\boldsymbol{m}_0$ for the first segment) and ending in a border (or in $\boldsymbol{m}_f$ for the last one). Then LPP (8) is applied on each of these segments.

Algorithm 1 computes the total time τ_f by using LPP in (8) for the linear trajectory ℓ from $\boldsymbol{m}_0$ to $\boldsymbol{m}_f$ which crosses $n \in \{1, 2, .., \gamma\}$ borders. In this algorithm, $\boldsymbol{m}_c^i$ stands for state at the intersection of ℓ and the i^{th} crossed border (starting from $\boldsymbol{m}_0$) $\ i \in \{1, 2, .., n\}$. Let $\boldsymbol{m}_c^0$ and $\boldsymbol{m}_c^{n+1}$ denote $\boldsymbol{m}_0$ and $\boldsymbol{m}_f$, respectively and $\boldsymbol{w}^i$ denote the flow obtained from the state $\boldsymbol{m}_c^i$ to the state $\boldsymbol{m}_c^{i+1}$. Note that, if ℓ does not cross any border, then $n = 0$, that is $\boldsymbol{m}_c^0 = \boldsymbol{m}_0$ and $\boldsymbol{m}_c^1 = \boldsymbol{m}_f$.

Algorithm 1 Linear trajectory

Input: $\langle \mathcal{N}, \boldsymbol{m}_0 \rangle, \ \ \boldsymbol{m}_f$
Compute the line ℓ connecting $\boldsymbol{m}_0$ and $\boldsymbol{m}_f$
Compute the intersection of ℓ and the crossed borders: $\boldsymbol{m}_c^1,\ \boldsymbol{m}_c^2,\ .....\boldsymbol{m}_c^n$
$\boldsymbol{m}_c^0 = \boldsymbol{m}_0,\ \ \boldsymbol{m}_c^{n+1} = \boldsymbol{m}_f$
for $i = 0$ to n **do**
  Determine τ_{i+1} by solving LPP in (8) with $\boldsymbol{m}_0 = \boldsymbol{m}_c^i$ and $\boldsymbol{m}_f = \boldsymbol{m}_c^{i+1}$
end for
Output: $\tau_1, \boldsymbol{w}^1, \tau_2, \boldsymbol{w}^2, ..., \tau_{n+1}, \boldsymbol{w}^{n+1}$, $\tau_f = \sum_{i=1}^{n+1} \tau_i$

Proposition 4. Let $\langle \mathcal{N}, \boldsymbol{\lambda}, \ \boldsymbol{m}_0 \rangle$ be a contPN system with $\boldsymbol{m}_0 > 0$. If $\boldsymbol{m}_f > 0$ belongs to $\mathcal{R}$:

- LPP(8) is feasible
- The control action given by Algorithm 1 ensures that $\boldsymbol{m}_f$ is reached in finite time.

Proof. Since $\boldsymbol{m}_f$ is a reachable marking, then there exists $\boldsymbol{x}$ such that the state equation 8(a) is satisfied. By taking τ_f sufficiently large 8(b) can be satisfied since $\lambda_j \cdot \Pi^z_{ji} \cdot \min\{m_{0i}, m_{fi}\} > 0$. Then, by (Júlvez et al. (2003)) the linear trajectory from $\boldsymbol{m}_0$ to $\boldsymbol{m}_f$ can be followed by the system since $\boldsymbol{m}_0 > 0$ and $\boldsymbol{m}_f > 0$, i.e. , all intermediate states are not spurious. Moreover, since $\boldsymbol{m}_f > 0$, by (Mahulea et al. (2008b)) $\boldsymbol{m}_f$ can be reached in finite time.

Example 5. Let us consider the control law design for the contPN in Example 2 (Figure 1). Assume the same $\boldsymbol{\lambda}$, $\boldsymbol{m}_0$ and $\boldsymbol{m}_f$. Note that the line ℓ connecting $\boldsymbol{m}_0$ and $\boldsymbol{m}_f$ crosses only one border: $m_2 = m_6$ and the crossing point is calculated as: $\boldsymbol{m}_c^1 = [7.33\ 4.67\ 4.33\ 1.67\ 1.33\ 4.67\ 4.33\ 2.67]^T$, $\boldsymbol{m}_c^0 = \boldsymbol{m}_0$, $\boldsymbol{m}_c^2 = \boldsymbol{m}_f$. The trajectory is illustrated in Figure 2 where the dotted line is the border between two regions. According to Algorithm 1, in the first iteration LPP (8)

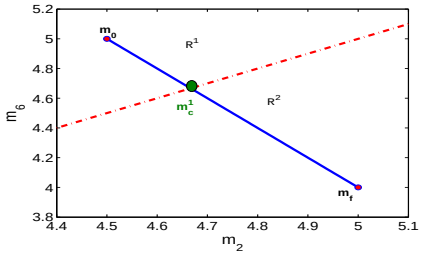

Fig. 2. Trajectory for Example 5

with $\boldsymbol{m}_0 = \boldsymbol{m}_c^0$ and $\boldsymbol{m}_f = \boldsymbol{m}_c^1$ is solved. Its constraints are:

$$\begin{aligned}
7.33 &= 7.5 + x_4 - x_1\\
4.67 &= 4.5 + x_1 - x_2\\
4.33 &= 4 + x_2 - x_3\\
1.67 &= 2 + x_3 - x_4\\
1.33 &= 1.5 + x_2 - x_1\\
4.67 &= 5 + x_3 - x_2\\
4.33 &= 4 + x_4 - x_3\\
2.67 &= 2.5 + x_2 + x_4 - x_1 - x_3
\end{aligned} \qquad (a)$$

$$\begin{aligned}
0 &\le x_1 \le 4 \cdot 1.33 \cdot \tau_f\\
0 &\le x_2 \le 4.5 \cdot \tau_f\\
0 &\le x_3 \le 3 \cdot 2.5\tau_f\\
0 &\le x_4 \le 1.66 \cdot \tau_f
\end{aligned} \qquad (b)$$

The optimal solution is $\tau_1 = 0.2$ t.u. and $w_1 = 2.49$, $w_2 = 1.67$, $w_3 = 0$, $w_4 = 1.67$. In the second iteration, i.e., $\boldsymbol{m}_0 = \boldsymbol{m}_c^1$ and $\boldsymbol{m}_f = \boldsymbol{m}_c^2$, the constraints are

$$\begin{aligned}
7 &= 7.33 + x_4 - x_1\\
5 &= 4.67 + x_1 - x_2\\
5 &= 4.33 + x_2 - x_3\\
1 &= 1.67 + x_3 - x_4\\
1 &= 1.33 + x_2 - x_1\\
4 &= 4.67 + x_3 - x_2\\
5 &= 4.33 + x_4 - x_3\\
3 &= 2.67 + x_2 + x_4 - x_1 - x_3
\end{aligned} \qquad (a)$$

$$\begin{aligned}
0 &\le x_1 \le 4 \cdot \tau_f\\
0 &\le x_2 \le 4 \cdot \tau_f\\
0 &\le x_3 \le 3 \cdot 2.67 \cdot \tau_f\\
0 &\le x_4 \le \tau_f
\end{aligned} \qquad (b)$$

The optimal solution is $\tau_2 = 0.67$ t.u. and $w_1 = 1.5$, $w_2 = 1$, $w_3 = 0$, $w_4 = 1$. The total time to go from $\boldsymbol{m}_0$ to $\boldsymbol{m}_f$ through the line ℓ is $\tau_f = 0.2 + 0.67 = 0.87$ t.u. And the obtained open loop control is:

$$\boldsymbol{u}(\tau) = \begin{cases} \begin{bmatrix} 4 \cdot m_5(\tau) - 2.49 \\ m_2(\tau) - 1.67 \\ 3 \cdot m_8(\tau) \\ m_4(\tau) - 1.67 \end{bmatrix}, \text{if } \ 0 \le \tau \le 0.2 \\ \\ \begin{bmatrix} 4 \cdot m_5(\tau) - 1.5 \\ m_2(\tau) - 1 \\ 3 \cdot m_8(\tau) \\ m_4(\tau) - 1 \end{bmatrix}, \text{if } \ 0.2 < \tau \le 0.87 \end{cases} \qquad (9)$$

Figure 3(a) illustrates the convergence of the marking m_1 under the designed control law, while Figure 3(b) shows the control signal u_1, w_1 and their upper bound.

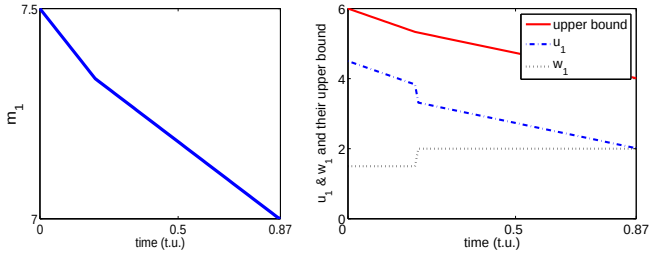

(a) (b)

Fig. 3. Evolution of (a) m_1 and (b) u_1, w_1 and and their upper bound for Example 5

4. REDUCING THE TIME BY COMPUTING A PIECEWISE LINEAR TRAJECTORY

Following Xu et al. (2008), this section makes use of intermediate state in order to improve the time duration to reach $\boldsymbol{m}_f$. From a technical point of view, the approach is different in the sense that the piecewise linear trajectory will use the borders of the regions and, possibly, inside regions the trajectory is refined recursively.

The designed control in the previous subsection takes the system from $\boldsymbol{m}_0$ to $\boldsymbol{m}_f$ through a linear trajectory by minimizing the time duration. In some cases, i.e., when the initial or final state have a small value, this may limit the speed of the response. In order to improve the time spent to move from $\boldsymbol{m}_0$ to $\boldsymbol{m}_f$, intermediate states denoted by $\boldsymbol{m}^k$ where $k \in \{1, 2...s\}$, that do not necessarily lie on the line from $\boldsymbol{m}_0$ to $\boldsymbol{m}_f$, are computed. The new trajectory is obtained as the union of $s+1$ linear segments: $\boldsymbol{m}_0 \to \boldsymbol{m}^1 \to \boldsymbol{m}^2 \to ... \to \boldsymbol{m}^s \to \boldsymbol{m}_f$. In order lighten the computation load, we consider the intermediate states in the range:

$$\mathcal{R}^I = \{\boldsymbol{m} \mid m_i \le \max\{m_{f_i}, m_{0_i}\},\ \ m_i \ge \min\{m_{f_i}, m_{0_i}\}, \\ i \in \{1, 2, .., |P|\}\}, \qquad (10)$$

Given that we assume that $\boldsymbol{m}_0$, $\boldsymbol{m}_f > 0$, all $\boldsymbol{m} \in \mathcal{R}^I$ are positive and reachable (Júlvez et al. (2003)). We will describe how to compute intermediate states that lie on the borders and in the interior of the regions, separately.

4.1 Intermediate states on the borders

Let the line from $\boldsymbol{m}_0$ to $\boldsymbol{m}_f$ cross s borders, and pass through $s+1$ different regions: $\mathcal{R}^1$, $\mathcal{R}^2$, ..., $\mathcal{R}^{s+1}$ with

corresponding constraint matrices $\mathbf{\Pi}^1$, $\mathbf{\Pi}^2 ... \mathbf{\Pi}^{s+1}$. We assign constant flows for each transitions during each line segments and the intermediate states on each border: $\boldsymbol{m}^1$, $\boldsymbol{m}^2 .... \boldsymbol{m}^s$. Under these assumptions, the following BLP with $\boldsymbol{m}^0 = \boldsymbol{m}_0$ and $\boldsymbol{m}^{s+1} = \boldsymbol{m}_f$ and with the variables $\boldsymbol{m}^1$, $\boldsymbol{m}^2$,....,$\boldsymbol{m}^{s-1}$, $\boldsymbol{m}^s$, τ_k , $\boldsymbol{x}^k = \boldsymbol{w}^k \cdot \tau_k$, $k \in \{1, ...s\}$ obtains the intermediate states that yield a minimum time for the piecewise linear trajectory:

$$\min \sum_{k=1}^{s+1} \tau_k$$

$$\boldsymbol{m}^{k+1} = \boldsymbol{m}^k + \boldsymbol{C} \cdot \boldsymbol{x}^{k+1}, \quad k \in \{0, 1, 2, .., s\} \qquad (a)$$

$$\left(\mathbf{\Pi}^k - \mathbf{\Pi}^{k+1}\right) \cdot \boldsymbol{m}^k = 0, \quad k \in \{1, 2, .., s\} \qquad (b)$$

$$m_i^k \leq m_i^{k+1} \text{ if } m_{0_i} \leq m_{f_i} \quad i \in \{1, 2..|P|\}, \quad k \in \{0, 1, 2, .., s\} \qquad (c)$$

$$m_i^k \geq m_i^{k+1} \text{ if } m_{0_i} \geq m_{f_i} \quad i \in \{1, 2..|P|\}, \quad k \in \{0, 1, 2, .., s\} \qquad (d)$$

$$0 \leq x_j^k \leq \lambda_j \cdot \Pi_{ji}^k \cdot \min\{m_i^{k-1}, m_i^k\} \cdot \tau_k, \text{ with } p_i \text{ st. } \Pi_{ji}^k \neq 0,\ j \in \{1, 2...|T|\}, \quad k \in \{1, 2..s\} \qquad (e)$$

(11)

The constraints correspond to (a) the time dependent equation to connect $\boldsymbol{m}^k$ to $\boldsymbol{m}^{k+1}$; (b) $\boldsymbol{m}^k$ is on the crossed border; (c & d) $\boldsymbol{m}^k$ is contained in the hypercube defined by the corners $\boldsymbol{m}^{k-1}$ and $\boldsymbol{m}^{k+1}$; (e) the constraints on the controlled flow.

4.2 Intermediate states inside regions

In the case that $\boldsymbol{m}_0$ and $\boldsymbol{m}_f$ are in the same region $\mathcal{R}^z$ a recursive method can be used to determine intermediate states in $\mathcal{R}^z$. In this method, we keep computing intermediate states until the time cannot be improved by a considerable amount. The same recursive method can also be applied to find additional intermediate states between $\boldsymbol{m}^k$ and $\boldsymbol{m}^{k+1}$, since they are on the borders of the same region. In this case, the BLP that will be solved in each step can be simplified to the following where $\boldsymbol{m}_0$ and $\boldsymbol{m}_f$ are known; τ_1, τ_2, $\boldsymbol{m}^d$, $\boldsymbol{x}^1 = \boldsymbol{w}^1 \cdot \tau_1, \boldsymbol{x}^2 = \boldsymbol{w}^2 \cdot \tau_2$ are variables:

$$\min\ \tau_1 + \tau_2$$

$$\boldsymbol{m}^d = \boldsymbol{m}_0 + \boldsymbol{C} \cdot \boldsymbol{x}^1$$
$$\boldsymbol{m}_f = \boldsymbol{m}^d + \boldsymbol{C} \cdot \boldsymbol{x}^2, \qquad (a)$$

$$\boldsymbol{m}^d = \boldsymbol{m}_0 + \boldsymbol{C} \cdot \boldsymbol{\sigma}, \quad \boldsymbol{m}^d,\ \boldsymbol{\sigma} \geq 0 \qquad (b)$$

$$\min\{m_{f_i}, m_{0_i}\} \leq m_i^d \leq \max\{m_{f_i}, m_{0_i}\}, \quad \forall i \in \{1, 2...|P|\} \qquad (c)$$

$$0 \leq x_j^1 \leq \lambda_j \cdot \Pi_{ji}^z \cdot \min\{m_{0_i}, m_i^d\} \cdot \tau_1, \text{ with } i \text{ st. } \Pi_{ji}^k \neq 0,\ j \in \{1, 2...|T|\}$$
$$0 \leq x_j^2 \leq \lambda_j \cdot \Pi_{ji}^z \cdot \min\{m_i^d, m_{f_i}\} \cdot \tau_2, \text{ with } i \text{ st. } \Pi_{ji}^k \neq 0,\ j \in \{1, 2...|T|\} \qquad (d)$$

(12)

Algorithm 2 expresses the recursive method we propose. It computes new intermediate states until the stopping criterion is satisfied: time of the trajectory cannot be decreased more than a given relative value ϵ. In the algorithm, *path* is a global variable storing the ordered set of couples of states in the trajectory and the relative times to reach them. The number of states in *path* is denoted by $size(path)$ and the i^{th} element of the set *path* is denoted by $path(i)$.

Algorithm 2 Piecewise Linear Trajectory

Input: $\langle \mathcal{N}, \boldsymbol{m}_0 \rangle$, $\boldsymbol{m}_f$, ϵ
Global variable: *path*
Compute the line ℓ connecting $\boldsymbol{m}_0$ and $\boldsymbol{m}_f$
Determine the number of crossed borders: s
if $s = 0$ **then**
  Solve (8) to obtain τ_f
  $path_0 = \{(\boldsymbol{m}_0, 0),\ (\boldsymbol{m}_f, \tau_f)\}$
else
  Solve (11) to obtain τ_f
  $path_0 = \{(\boldsymbol{m}_0, 0),\ (\boldsymbol{m}^1, \tau_1), ..., (\boldsymbol{m}_f, \tau_f)\}$
end if
$\tau_x = \tau_f$, $path = path_0$
for $i = 1 : size(path_0) - 1$ **do**
  $(\boldsymbol{m}^x, \tau_x) = path_0(i)$, $(\boldsymbol{m}^y, \tau_y) = path_0(i+1)$
  Call **Split**$((\boldsymbol{m}^x, \tau_x),\ (\boldsymbol{m}^y, \tau_y),\ \epsilon)$
end for
Calculate the total time for *path*, i.e., τ_y
Output:*path*

Split$((\boldsymbol{m}^x, \tau_x),\ (\boldsymbol{m}^y, \tau_y),\ \epsilon)$
  Solve (12) to obtain $\tau_1,\ \tau_2,\ \boldsymbol{m}^d$
  if $\dfrac{\tau_y - (\tau_1 + \tau_2)}{\tau_y} > \epsilon$ **then**
    Insert $(\boldsymbol{m}^d, \tau_1)$ in *path*
    Change $(\boldsymbol{m}^y, \tau_y)$ in *path* by $(\boldsymbol{m}^y, \tau_2)$
    Call **Split**$((\boldsymbol{m}^x, \tau_x),\ (\boldsymbol{m}^d, \tau_1),\ \epsilon)$
    Call **Split**$((\boldsymbol{m}^d, \tau_1),\ (\boldsymbol{m}^y, \tau_2),\ \epsilon)$
  end if

Example 6. Let us consider once again the contPN system in Example 5 (Figure 1). Since the linear trajectory between $\boldsymbol{m}_0$ and $\boldsymbol{m}_f$ crosses only one border, $s = 1$ and solving (11) with $s = 1$ yields 0.83 t.u. as a total time. And the new path is $\boldsymbol{m}_0 \rightarrow \boldsymbol{m}^1 \rightarrow \boldsymbol{m}_f$, where $\boldsymbol{m}^1 = [7.5\ 4.5\ 4.5\ 1.5\ 1.5\ 4.5\ 4.5\ 3]^T$. For an additional intermediate state, say $\boldsymbol{m'}^1$, between $\boldsymbol{m}_0$ and $\boldsymbol{m}^1$, we solve (12) for $\boldsymbol{m}_0 = [7.5\ 4.5\ 4\ 2\ 1.5\ 5\ 4\ 2.5]^T$ and $\boldsymbol{m}_f = \boldsymbol{m}^1$. Similarly, for an additional intermediate state between $\boldsymbol{m}^1$ and $\boldsymbol{m}_f$, say $\boldsymbol{m'}^2$, we solve (12) for $\boldsymbol{m}_0 = \boldsymbol{m}^1$ and $\boldsymbol{m}_f = [7\ 5\ 5\ 1\ 1\ 4\ 5\ 3]^T$. And the new path $\boldsymbol{m}_0 \rightarrow \boldsymbol{m'}^1 \rightarrow \boldsymbol{m}^1 \rightarrow \boldsymbol{m'}^2 \rightarrow \boldsymbol{m}_f$ is obtained, where:

$$\boldsymbol{m'}^1 = [7.5\ 4.5\ 4.26\ 1.74\ 1.5\ 4.74\ 4.26\ 2.76]^T$$

and

$$\boldsymbol{m'}^2 = [7.45\ 4.78\ 4.55\ 1.22\ 1.22\ 4.45\ 4.78\ 3]^T.$$

The total time is reduced to 0.74 t.u. with the control action $u(\tau) = [4 \cdot m_5(\tau) - 1.74 \quad m_2(\tau) - 1.74 \quad 3 \cdot m_8(\tau) \quad m_4(\tau) - 1.74]^T$ for $0 \leq \tau \leq 0.15$; $u(\tau) = [4 \cdot m_5(\tau) - 1.74 \quad m_2(\tau) - 1.74 \quad 3 \cdot m_8(\tau) \quad m_4(\tau) - 1.75]^T$ for $0.15 \leq \tau \leq 0.29$; $u(\tau) = [4 \cdot m_5(\tau) - 1.43 \quad m_6(\tau) - 0.21 \quad 3 \cdot m_8(\tau) \quad m_4(\tau) - 1.22]^T$ for $0.3 \leq \tau \leq 0.52$;

$u(\tau) = [4 \cdot m_5(\tau) - 3.04 \;\; m_6(\tau) - 2.04 \;\; 3 \cdot m_8(\tau) \;\; m_4(\tau) - 1]^T$ for $0.52 \leq \tau \leq 0.74$. The trajectories for one and three intermediate states are illustrated in Figure 4(a) and 4(b), respectively. In these figures the dotted line shows the border between $\mathcal{R}^1$ and $\mathcal{R}^2$. The total time duration for

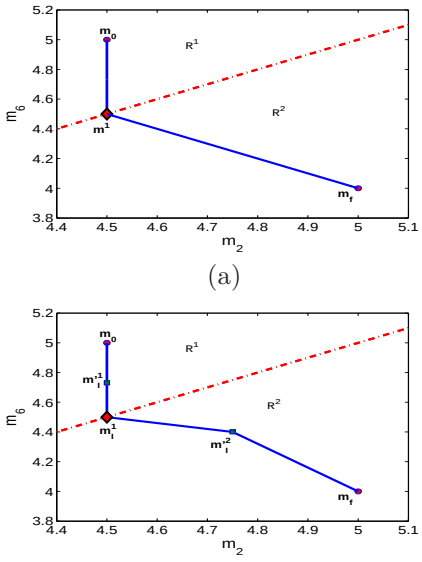

(a)

(b)

Fig. 4. Trajectory for (a)1 int. state and (b)3 int. state for Example 6

several intermediate states can be found in Table 1. The experiments were performed by a Matlab program running on a PC with Intel(R) Core(TM)2CPU T5600 @ 1.83GHz, 2.00 GB of RAM.

Table 1. Intermediate States

Number of int. states	0	1	3	9	13
Total duration (t.u.)	0.87	0.83	0.74	0.73	0.72
CPU time (sec.)	0.03	0.11	0.32	1.65	2.32

5. CLOSED LOOP CONTROL

Using Algorithm 2 we obtain an open loop controller. Obviously, in a real system, perturbations affect the evolution and when the control law is implemented, such perturbations must be handled to minimize their effect. In this section we assume that the PWL trajectory $path = \{\boldsymbol{m}_0, \; \boldsymbol{m'}^1, ..., \boldsymbol{m'}^s, \; \boldsymbol{m}_f\}$ has been computed using Algorithm 2. The online implementation proposed in this section follows this trajectory by calculating a new state after each time step.

For the online implementation we consider the discrete-time representation of the system (Mahulea et al. (2008a)). Our approach will be: for each segment of trajectory, during each discrete-step k we will apply the maximum possible flow obtained by solving a LPP. The procedure is a closed loop control and in fact, can be seen as a model predictive control scheme with timing horizon 1 and having as optimization index the minimization of the time. In (Mahulea et al. (2008a)) it is proved that using this control scheme the closed loop system is asymptotically stable.

The discrete-time representation of the continuous-time system (6) is given by:

$$\begin{array}{l} \boldsymbol{m}(k+1) = \boldsymbol{m}(k) + \Theta \cdot \boldsymbol{C} \cdot \boldsymbol{w}(k) \\ 0 \leq \boldsymbol{w}(k) \leq \boldsymbol{\Lambda} \cdot \boldsymbol{\Pi}(\boldsymbol{m}(k)) \cdot \boldsymbol{m}(k) \end{array} \tag{13}$$

Here Θ is the sampling period ($\tau = k \cdot \Theta$) and $\boldsymbol{m}(k)$ is the marking at step k, i.e., at time $k \cdot \Theta$. The sampling period should be small enough to avoid spurious states. For all p in P the following should be satisfied (Mahulea et al. (2008a)):

$$\sum_{t_j \in p^\bullet} \lambda_j \cdot \Theta < 1 \tag{14}$$

In order to design the closed loop control for *path* (see output of Algorithm 2), Algorithm 3 is developed. Here s denotes the number of intermediate states. In the algorithm, the procedure is applied to each segment ($\boldsymbol{m'}^j$, $\boldsymbol{m'}^{j+1}$) of the *path*. Therefore, the first problem will be to reach $\boldsymbol{m'}^1$ from $\boldsymbol{m}_0$. In order to do this, LPP (15) computes at $k \cdot \Theta$ the maximum distance that can be executed from the actual marking, $\boldsymbol{m}(k)$, in the direction of $\boldsymbol{m'}^{j+1}$ during the next Θ t.u. This LPP tries to maximize the distance during the next Θ that can be executed from the actual marking (constraint 1) such that the obtained intermediate marking $\boldsymbol{m'}_{next}$ belongs to the straight line from the actual marking $\boldsymbol{m}(k)$ to the final one $\boldsymbol{m'}^{j+1}$ (constraints 2 and 3) while the controlled flow is dynamically bounded (constraint 4). Then the same procedure is applied when the initial marking is $\boldsymbol{m'}^1$ and $\boldsymbol{m'}^2$ should be reached and so on. The procedure stops when a marking sufficiently close to $\boldsymbol{m}_f$ is reached. We will denote by $\boldsymbol{z}$ the perturbation that affects the flow (see equation (16)).

If there is no perturbation, the total time to reach the desired marking by closed loop procedure can be smaller than the time obtained by the open loop procedure. This is due to the fact that the flow in the open loop control that drive the system from a marking $\boldsymbol{m'}^j$ to a marking $\boldsymbol{m'}^{j+1}$ is constant and it is bounded by these two markings. In the closed loop implementation, the flow at step k is bounded by the actual marking and $\boldsymbol{m'}^{j+1}$. Obviously, being the actual marking a convex combination of $\boldsymbol{m'}^j$ and $\boldsymbol{m'}^{j+1}$ the flow may be greater. On the other hand, because of discrete time implementation, the time of the closed loop control can be greater in some cases. For example, let us assume that the optimal time computed by the offline controller to go from $\boldsymbol{m'}^j$ to $\boldsymbol{m'}^{j+1}$ is 0.3 t.u. Taking a sampling time equal to 0.25 and assuming a maximum flow during trajectory equal to 1, in the absence of any perturbation, at least two steps are required to reach the desired marking. This corresponds to, at least, 0.5 t.u. what is greater than the time given by the open loop controller (which is 0.3 t.u.).

Example 7. Let us consider the contPN system considered in Example 6 (Figure 1) with the same initial and target marking: $\boldsymbol{m}_0 = [7.5 \;\; 4.5 \;\; 4 \;\; 2 \;\; 1.5 \;\; 5 \;\; 4 \;\; 2.5]^T$ and $\boldsymbol{m}_f = [7 \;\; 5 \;\; 5 \;\; 1 \;\; 1 \;\; 4 \;\; 5 \;\; 3]^T$. In Example 6, *path* was obtained as $path = \{\boldsymbol{m}_0, \; \boldsymbol{m'}^1, \; \boldsymbol{m'}^2, \; \boldsymbol{m'}^3, \; \boldsymbol{m}_f\}$ where $\boldsymbol{m'}^1 = [7.5 \;\; 4.5 \;\; 4.26 \;\; 1.74 \;\; 1.5 \;\; 4.74 \;\; 4.26 \;\; 2.76]^T$, $\boldsymbol{m'}^2 = [7.5 \;\; 4.5 \;\; 4.5 \;\; 1.5 \;\; 1.5 \;\; 4.5 \;\; 4.5 \;\; 3]^T$ and $\boldsymbol{m'}^3 = [7.45 \;\; 4.78 \;\; 4.55 \;\; 1.22 \;\; 1.22 \;\; 4.45 \;\; 4.78 \;\; 3]^T$.

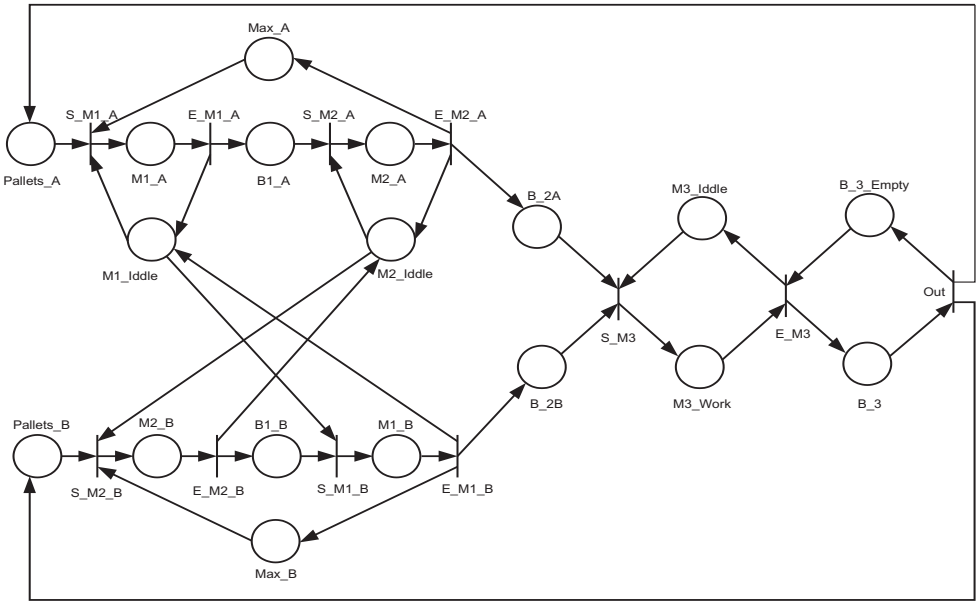

Fig. 5. A contPN model of a flexible manufacturing system

Algorithm 3 Closed Loop Control

Input: $\langle \mathcal{N}, \boldsymbol{m}_0 \rangle$, $\boldsymbol{m}_f$, $path$, s, ρ
$\boldsymbol{m'}^0 = \boldsymbol{m}_0$; $\boldsymbol{m'}^{s+1} = \boldsymbol{m}_f$;
$\boldsymbol{m}(0) = \boldsymbol{m'}^0$; $k = 0$;
for $j = 0$ to s **do**
  while $\frac{||\boldsymbol{m}(k) - \boldsymbol{m'}^{j+1}||}{||\boldsymbol{m}(k)||} > \rho$ **do**
    Solve the following LPP

$$\begin{aligned} \max\ & \alpha \\ \text{s.t.}\ & \boldsymbol{m'}_{next} = \boldsymbol{m}(k) + \Theta \cdot \boldsymbol{C} \cdot \boldsymbol{w} \\ & \boldsymbol{m'}_{next} = (1-\alpha) \cdot \boldsymbol{m}(k) + \alpha \cdot \boldsymbol{m'}^{j+1} \\ & 0 \le \alpha \le 1 \\ & 0 \le \boldsymbol{w} \le \boldsymbol{\Lambda} \cdot \boldsymbol{\Pi}(\boldsymbol{m}(k)) \cdot min\{\boldsymbol{m}(k), \boldsymbol{m'}_{next}\} \end{aligned} \tag{15}$$

    Advance one step and obtain the new marking

$$\boldsymbol{m}(k+1) = \boldsymbol{m}(k) + \Theta \cdot \boldsymbol{C} \cdot (\boldsymbol{w} + \boldsymbol{z}) \tag{16}$$

    $k = k + 1$
  end while
end for

According to inequality (14), $\Theta \le 1/7$ must be satisfied. Let us assume that $\Theta = 0.01$ and no perturbation. According to Algorithm 3, we consider first the segment $(\boldsymbol{m}_0, \boldsymbol{m'}^1)$. That is, LPP (15) is solved at $k = 0$ to calculate the maximum distance that can be executed from $\boldsymbol{m}_0$ during Θ t.u in the direction of $\boldsymbol{m'}^1$. This yields $\boldsymbol{w}(1) = [2.02\ 2.02\ 0\ 2.02]^T$. Applying the corresponding control to the system $\boldsymbol{m}(1) = [7.5\ 4.5\ 4.02\ 1.98\ 1.5\ 4.98\ 4.02\ 2.52]^T$ is reached.

Let $\rho = 10^{-2}$, then since $\frac{||\boldsymbol{m}(1) - \boldsymbol{m'}^1||}{||\boldsymbol{m}(1)||} > \rho$, LPP(15) is solved considering $\boldsymbol{m}(1)$ the initial marking. The obtained controlled flow is $\boldsymbol{w}(2) = [1.99\ 1.99\ 0\ 1.99]^T$ corresponding to $\boldsymbol{m}(2) = [7.5\ 4.5\ 4.04\ 1.96\ 1.5\ 4.96\ 4.04\ 2.54]^T$.

After the execution of Algorithm 3, $\boldsymbol{m}_f$ is reached from $\boldsymbol{m}_0$ after 66 discrete steps which correspond to 0.66 t.u. This is smaller than the time obtained by the open loop computation which was 0.74 t.u.

6. CASE STUDY

In this section we will apply our heuristic method for minimum time control to a manufacturing system. The net in Figure 5 (Zimmermann et al. (2001)) represents a flexible manufacturing system. Let us assume the speed of all operations take 1 t.u., i.e., $\boldsymbol{\lambda} = \boldsymbol{1}$. A product is composed from two different parts, A and B. Parts A are processed in machine $M1$ and then in machine $M2$ while parts B are processed in machine M2 and after in machine $M1$. The intermediate products are stored in B_1A and B_1B, and the final products respectively in B_2A and B_2B. Machine $M3$ assembles parts A and parts B producing in this way the final product which is temporally stored in B_3. The parts are moved on pallets. Hence, in this system we have 3 sequential machines, 4 intermediate deposits and one terminal deposit.

Let us assume that initially, there are 35 pallets of type A ($\boldsymbol{m}_0[Pallets\_A] = 35$); 25 pallets of type B ($\boldsymbol{m}_0[Pallets\_B] = 25$); one machine of each type from which the first two are initially in *Idle* state, while the third one is in *working* state ($\boldsymbol{m}_0[M1\_Iddle] = \boldsymbol{m}_0[M2\_Iddle] = \boldsymbol{m}_0[M3\_Work] = 1$); one final product of type A and one of type B produced ($\boldsymbol{m}_0[B\_2A] = \boldsymbol{m}_0[B\_2B] = 1$); a maximum of 10 parts of type A and B can be produced at each time ($\boldsymbol{m}_0[Max\_A] = \boldsymbol{m}_0[Max\_B] = 10$); and finally, the capacity of the buffer to store the final products just before the recycling of pallets is equal to 25 ($\boldsymbol{m}_0[B\_3\_Empty] = 25$). Let us consider the task of producing 10 final product as fast as possible, i.e., in minimum time. Let the final marking for this control goal be: $\boldsymbol{m}_f[Pallets\_A] = 27$, $\boldsymbol{m}_f[Pallets\_B] = 17$, $\boldsymbol{m}_f[Max\_A] = \boldsymbol{m}_f[Max\_B] = 10$, $\boldsymbol{m}_f[M1\_Iddle] = \boldsymbol{m}_f[M2\_Iddle] = \boldsymbol{m}_f[M3\_Iddle] = 1$, $\boldsymbol{m}_f[B\_3\_Empty] = 15$ and $\boldsymbol{m}_f[B\_3] = 10$. As previously established, it is assumed that the initial and target markings are strictly positive, i.e. , $m_0(p), m_f(p) \ge \mu$. In this example $\mu = 0.01$. Driving the system from $\boldsymbol{m}_0$ to $\boldsymbol{m}_f$ through the linear trajectory (see LPP (8)) by assigning constant flows to transitions takes 1000 t.u.

Table 2. Intermediate States

place	$\boldsymbol{m}_0$	$\boldsymbol{m}'^1$	$\boldsymbol{m}'^2$	$\boldsymbol{m}'^3$	$\boldsymbol{m}'^4$	$\boldsymbol{m}_f$
Pallet_A	35.0100	33.5000	31.0000	30.0000	28.5008	27.0000
M1_A	0.0100	0.0100	0.0100	0.0100	0.0100	0.0100
B1_A	0.0100	0.0100	0.0100	0.0100	0.0100	0.0100
M2_A	0.0100	0.0100	0.0100	0.0100	0.0100	0.0100
MAX_A	10.0100	10.0000	10.0000	10.0000	10.0000	10.0000
M1_IDLE	1.0000	1.0000	1.0000	1.0000	1.0000	1.0000
M2_IDLE	1.0000	1.0000	1.0000	1.0000	1.0000	1.0000
Pallet_B	25.0100	23.5000	21.0000	20.0000	18.5008	17.0000
M2_B	0.0100	0.0100	0.0100	0.0100	0.0100	0.0100
B1_B	0.0100	0.0100	0.0100	0.0100	0.0100	0.0100
M1_B	0.0100	0.0100	0.0100	0.0100	0.0100	0.0100
Max_B	10.0100	10.0000	10.0000	10.0000	10.0000	10.0000
B2_A	1.0100	1.0100	0.5100	0.0149	0.0100	0.0100
B2_B	1.0100	1.0100	0.5100	0.0149	0.0100	0.0100
M3_Idle	0.0100	0.5100	0.5100	1.0001	1.0099	1.0100
M3_Work	1.0100	0.5100	0.5100	0.0199	0.0101	0.0100
B3_Empty	25.0100	23.0000	20.0000	18.0148	16.5009	15.0000
B_3	0.0100	2.0100	5.0100	6.9952	8.5091	10.0100

In order to improve the time and refine the trajectory, we apply Algorithm 2 with $\epsilon = 10^{-3}$. The resulting path is composed by 4 intermediate states. Therefore 5 line segments, i.e., $path = \{\boldsymbol{m}_0 \rightarrow \boldsymbol{m}'^1 \rightarrow \boldsymbol{m}'^2 \rightarrow \boldsymbol{m}'^3 \rightarrow \boldsymbol{m}'^4 \rightarrow \boldsymbol{m}_f\}$ (see Table 2) are obtained. The time spent through this PWL trajectory is 802 t.u. The controlled flows, $\boldsymbol{w}$, at each segment are given in Table 3.

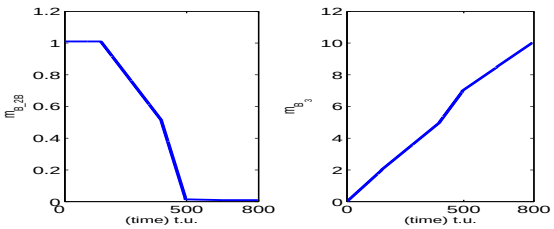

Fig. 6. Evolution of m_{B_2B} and m_{B_3}

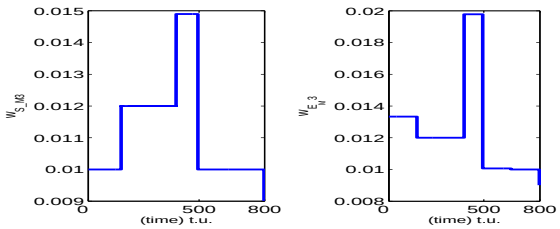

Fig. 7. Evolution of w_{S_M3} and w_{E_M3}

Applying the closed loop control developed in Section 5 assuming $\Theta = 0.01$ which satisfies inequality (14) and no perturbation, the total time to drive the system from $\boldsymbol{m}_0$ to $\boldsymbol{m}_f$ through the path is obtained as 800 t.u. Under closed loop control, the evolution of markings of places B_2B and B_3; and the controlled flows of transitions S_M3, E_M3 are shown in Figure 6 and Figure 7, respectively.

In order to see the effect of the perturbation on the closed loop controlled system, we introduce a perturbation on the flow of transitions E_M1_B, S_M3, E_M3 and Out during the time intervals [0 150] [300 400]. The perturbation applied to transitions S_M3, E_M3, i.e. z_{S_M3}, z_{E_M3} (see equation (16)), is shown in Figure 8.

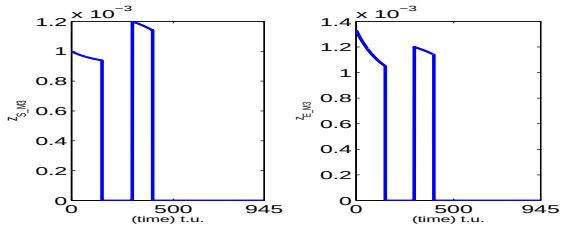

Fig. 8. Perturbation effect on transitions z_{S_M3} and z_{E_M3}

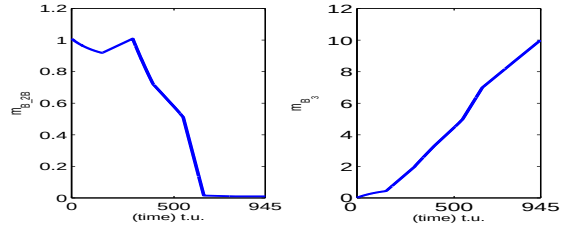

Fig. 9. Evolution of m_{B_2B} and m_{B_3} under perturbation effect

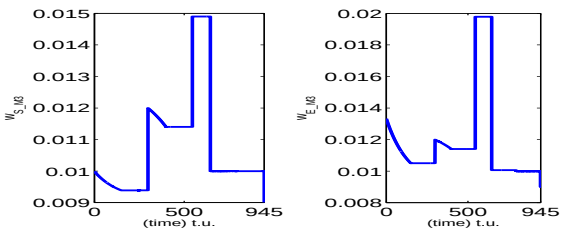

Fig. 10. Evolution of w_{S_M3} and w_{E_M3} under perturbation effect

Under this noisy condition, when the closed loop control is applied, the total time is obtained as 945 t.u. The evolution of markings of places B_2B and B_3, and the controlled flows of transitions S_M3, E_M3 are shown in Figure 9 and Figure 10, respectively.

Table 3. Controlled flows

transition	$(\boldsymbol{m}_0,\ \boldsymbol{m}'^1)$	$(\boldsymbol{m}'^1,\ \boldsymbol{m}'^2)$	$(\boldsymbol{m}'^2,\ \boldsymbol{m}'^3)$	$(\boldsymbol{m}'^3,\ \boldsymbol{m}'^4)$	$(\boldsymbol{m}'^4,\ \boldsymbol{m}_f)$
S_M1_A	0.0100	0.0100	0.0100	0.0099	0.0100
E_M1_A	0.0100	0.0100	0.0100	0.0099	0.0100
S_M2_A	0.0100	0.0100	0.0100	0.0099	0.0100
E_M2_A	0.0100	0.0100	0.0100	0.0099	0.0100
S_M2_B	0.0100	0.0100	0.0100	0.0099	0.0100
E_M2_B	0.0100	0.0100	0.0100	0.0099	0.0100
S_M1_B	0.0100	0.0100	0.0100	0.0099	0.0100
E_M1_B	0.0100	0.0100	0.0100	0.0099	0.0100
S_M3	0.0100	0.0120	0.01495	0.0100	0.0100
E_M3	0.0140	0.0120	0.01985	0.0100	0.0100
Out	0.0000	0.0000	0.0000	0.0000	0.0000

7. CONCLUSIONS

The control problem addressed in this paper consists of reaching a target state by approaching minimum time through a piecewise linear trajectory. Besides the piecewise linear dynamics of continuous Petri nets, the control method handles the fact that the input constraints depend on the current marking, i.e., the inputs are dynamically constrained.

The method proposed in this paper computes first a "rough" piecewise linear trajectory that is refined afterwards in those intervals that allow an improvement. The heuristics makes use of BLPs to obtain intermediate states and LPPs to compute linear trajectories. The refinement of the trajectory is achieved recursively. Finally, in a similar way to a receding horizon scheme, we proposed a closed loop method that ensures that the final marking is reached.

The approach presented in this paper has a relatively low complexity compared to previous works and thanks to the possibility of performing trajectory refinements it produces close to optimal results in general. This feature together with the fact of being embedded in a close loop scheme makes it feasible for large plants suffering from noisy measures.

REFERENCES

Apaydin-Ozkan, H., Júlvez, J., Mahulea, C., and Silva, M. (2009). An Efficient Heuristics for Minimum Time Control of Continuous Petri nets. In 3^{rd} *IFAC Conference on Analysis and Design of Hybrid Systems (ADHS 2009)*, 44–49. Zaragoza, Spain.

Balduzzi, F., Giua, A., and Menga, G. (2000). First-Order Hybrid Petri Nets: a Model for Optimization and Control. *IEEE Trans. on Robotics and Automation*, 16(4), 382–399.

Bemporad, A. and Morari, M. (1999). Control of systems integrating logic, dynamics, and constraints. *Automatica*, 35(3), 407–427.

David, R. and Alla, H. (2005). *Autonomous and timed continuous Petri nets*. Springer, Berlin.

Habets, L., Collins, P., and van Schuppen, J. (2006). Reachability and control synthesis for piecewise-affine hybrid systems on simplices. *Automatic Control, IEEE Transactions on*, 51(6), 938–948. doi:10.1109/TAC.2006.876952.

Júlvez, J., Recalde, L., and Silva, M. (2003). On reachability in autonomous continuous Petri net systems. In W. van der Aalst and E. Best (eds.), 24^{th} *International Conference on Application and Theory of Petri Nets (ICATPN 2003)*, volume 2679 of *Lecture Notes in Computer Science*, 221–240. Springer, Eindhoven, The Netherlands.

Mahulea, C., Giua, A., Recalde, L., Seatzu, C., and Silva, M. (2008a). Optimal model predictive control of timed continuous Petri nets. *IEEE Transactions on Automatic Control*, 53(7), 1731 – 1735.

Mahulea, C., Ramirez, A., Recalde, L., and M.Silva (2008b). Steady state control reference and token conservation laws in continuous Petri net systems. *IEEE Transactions on Automation Science and Engineering*, 5(2), 307–320.

Mahulea, C., Recalde, L., and Silva, M. (2009). Basic Server Semantics and Performance Monotonicity of Continuous Petri Nets. *Discrete Event Dynamic Systems: Theory and Applications*, 19(2), 189 – 212.

Montagner, V.F., Leite, V., Oliveira, R., and Peres, P. (2006). State feedback control of switched linear systems: An LMI approach. *Journal of Computational and Applied Mathematics*, 94(2), 192–206.

Silva, M. and Recalde, L. (2004). On fluidification of Petri net models: from discrete to hybrid and continuous models. *Annual Reviews in Control*, 28(2), 253–266.

Xu, J., Recalde, L., and Silva, M. (2008). Tracking control of timed continuous Petri net systems under infinite servers semantics. In *17th World Congress of IFAC*, 3192–3197. Seoul, Korea.

Yang, H., Xie, G., Chu, T., and Wang, L. (2006). Commuting and stable feedback design for switched linear systems. *Journal of Computational and Applied Mathematics*, 94(2), 192–206.

Zhou, M., DiCesare, F., and Guo, D. (1990). Modeling and performance analysis of a resource-sharing manufacturing system using stochastic Petri nets. In *Fifth IEEE Symp. on Intelligent Control*, 1005–1010. Phildephia, PA.

Zimmermann, A., Rodríguez, D., and Silva, M. (2001). A Two Phase Optimisation Method for Petri Net Models of Manufacturing Systems. *Journal of Intelligent Manufacturing*, 12(5), 421–432.